

Sound propagation in gas-filled rigid framed porous media : general theory and new experimental and numerical data

Denis Lafarge*, Michel Henry*, Mouaouia Firdaouss†, Jean-Luc Guermond‡

*LAUM, (URA CNRS 6613), Institut d'Acoustique et de Mécanique, Avenue O. Messiaen, BP535, 72017 Le Mans Cedex (France), †LIMSI, (UPR CNRS 3251), BP 133, 91403, Orsay (France), and UFR 23, UPMC Paris VI, Paris (France), ‡LIMSI, (UPR CNRS 3251), BP 133, 91403, Orsay (France)

Abstract: Modelling sound propagation in gas-filled rigid porous media, it is customary to introduce a complex density $\tilde{\rho}$ and a complex compressibility \tilde{K} . The two functions of the angular frequency ω depend on the geometry of the porous domain and determine the characteristic impedance $\tilde{Z} = (\tilde{\rho}\tilde{K})^{1/2}$ and propagation constant $\tilde{q} = \omega(\tilde{\rho}/\tilde{K})^{1/2}$. Here we review the general theory of functions $\tilde{\rho}$ and \tilde{K} , and provide new data illustrating the validity of scaling laws inspired by the work by Avellaneda and Torquato [1], Johnson et al. [2], Pride et al. [3] and Champoux and Allard [4].

GENERAL THEORY

In the gas-saturated porous medium, one distinguishes the microscopic level where gas motion occur according to the compressible Navier-Stokes/Fourier model of linear acoustics, and the macroscopic level where

$$-i\omega\tilde{\rho} \langle \mathbf{v} \rangle = -\nabla \langle p \rangle \quad (1), \quad \frac{-i\omega}{\tilde{K}} \langle p \rangle = -\nabla \cdot \langle \mathbf{v} \rangle \quad (2).$$

with $\langle \mathbf{v} \rangle$ and $\langle p \rangle$ the averaged velocity and excess pressure. (Isotropy is assumed, so that $\tilde{\rho}$ is a scalar).

Assuming a wide separation between the microscopic and macroscopic lengthscales, a straightforward application of the homogenization technique [5] yields two different microscopic boundary value problems to be solved. One of these describes the (velocity) response of a viscous incompressible fluid subject to an applied uniform macroscopic pressure gradient. It determines $\tilde{\rho}$. The other describes the (excess temperature) response of a thermal fluid subject to an applied uniform excess pressure. It determines \tilde{K} . The vanishing of velocity and excess temperature fields at the pore walls is assumed. Finally, $\tilde{\rho}$ and \tilde{K} can be formally expressed as

$$\frac{\tilde{\rho}}{\rho} = \frac{1}{\alpha_\infty} (1 - \tilde{\chi}(\omega)) \quad (3), \quad \frac{\tilde{K}}{K} = 1 + (\gamma - 1)\tilde{\chi}'(\omega) \quad (4).$$

where ρ and K are the ambient density and adiabatic bulk modulus, γ is the specific heat ratio, the dimensionless constant α_∞ is the tortuosity [2] and $\tilde{\chi}(\omega)$ and $\tilde{\chi}'(\omega)$ are complex relaxation functions :

$$\tilde{\chi}(\omega) = \int \frac{dG(\Theta)}{1 - i\omega\Theta} \quad (5), \quad \tilde{\chi}'(\omega) = \int \frac{dG'(\Theta)}{1 - i\omega\Theta} \quad (6)$$

which tend to one in the low-frequency limit and to zero in the high frequency limit. The distributions $G(\Theta)$ and $G'(\Theta)$ are known in principle once the gas domain and its boundary surfaces solid/gas are specified. The precise definition of $G(\Theta)$, related to the Stokes operator, was given by Avellaneda and Torquato [1], Eq. (81). We note that the distribution $G'(\Theta)$ is similarly related to the Laplace operator. In practice, we cannot solve for the complete set of solutions of the Stokes and Laplace operators in the complicated microgeometry, and the distributions $G(\Theta)$ and $G'(\Theta)$ remain to some extent unknown. In this paper we extend the work by Johnson *et al.* and Pride *et al.* and propose that the functions $\tilde{\chi}(\omega)$ and $\tilde{\chi}'(\omega)$ be described as :

$$1/\chi(\omega) = 1 - ix/S(x) \quad (7), \quad 1/\chi'(\omega) = 1 - ix'/S'(x') \quad (8),$$

with $S(x) = 1 - P + P(1 - ixM/2P^2)^{1/2}$, $S'(x') = 1 - P' + P'(1 - ix'M'/2P'^2)^{1/2}$ and $x = \omega Fk_0/\nu$, $x' = \omega F'k'_0/\nu'$. Here, ν is the kinematic viscosity and ν' is ν divided by the Prandtl number, $F = \alpha_\infty/\phi$ is the formation factor, $F' = 1/\phi$ is the inverse porosity, k_0 is the Darcy permeability, k'_0 is the inverse trapping constant of the porous medium [5,1]. The dimensionless form factors M and M' are defined through the relations $M = 8Fk_0/\Lambda^2$, $M' = 8F'k'_0/\Lambda^2$. Additionnal form factors $P = M/4(\alpha_0/\alpha_\infty - 1)$ and $P' = M'/4(\alpha'_0 - 1)$ are introduced in order to ensure the low-frequency conditions $\text{Re}(\tilde{\rho}/\rho) \rightarrow \alpha_0$ and $\gamma - \text{Re}(K/\tilde{K}) \rightarrow (\gamma - 1)/\alpha'_0$ for $\omega \rightarrow 0$.

Eqs.(7) and (8) with the definitions therein and the simplifications $P=1$ and $P'=1$ correspond to the simple scaling function proposed by Johnson *et al.* [2] and its extension to thermal effects [5]. The more general expression (7) with $P \neq 1$ was previously given by Pride *et al.* [3] (Eq. 94). Two examples, one numerical and one experimental, illustrate the accuracy of the modelling

NUMERICAL AND EXPERIMENTAL EXAMPLES

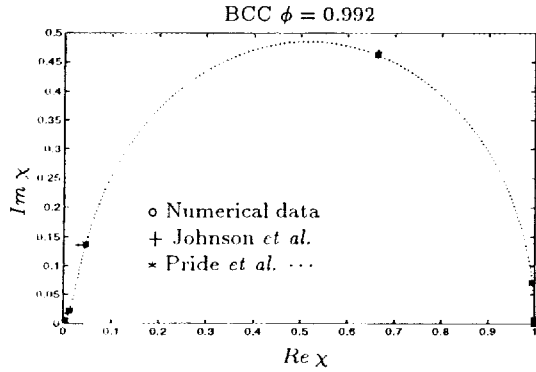


FIGURE 1a

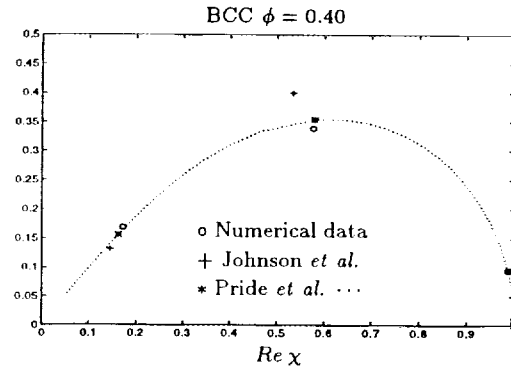


FIGURE 1b

Detailed numerical results for the dynamic permeability $\tilde{k}(\omega) = v\phi\rho / -i\omega\tilde{p}(\omega)$ have been presented by Chapman and Higdon [6] for periodic lattices of spheres (SC, BCC, FCC), ranging from dilute systems with isolated spheres to highly concentrated consolidated media with overlapping spheres. On Figures 1a and 1b, comparisons between the numerical data in [6] and the Johnson *et al.* and Pride *et al.* scaling functions for the BCC case, are given for two porosities in the form of Cole-Cole plots. A very precise agreement with Pride *et al.* modelling is apparent. In the case of dilute spheres ($\phi = 0.992$) the relaxation function $\tilde{\chi}(\omega)$ tends to the simple "Debye form" $1/(1 - i\omega Fk_0 / v)$. The case of intermediate porosities ($\phi = 0.40$) is close to the "Davidson-Cole" form with exponent $1/2$.

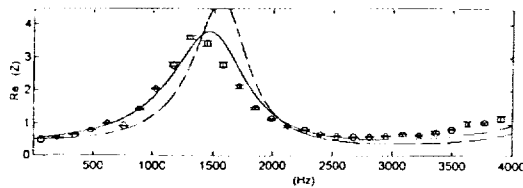


FIGURE 2a

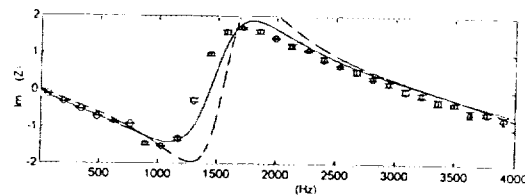


FIGURE 2b

Precise acoustical tests of the modelling have been performed on different polyurethane porous foams of moderate flow resistivity. An example is given in Figure 2 where the reduced surface impedance of a hard baked porous foam of thickness 4.4 cm and permeability $3.9 \cdot 10^{-9} \text{ m}^2$ is measured in a tube with the TMTC technique (two microphones, three calibrations) [8], and compared with predictions. All parameters F , k_0 , α_0 , Λ , F' , k'_0 , α'_0 , Λ' were independently measured. The flow resistivity and porosity are measured using standard techniques. Ultrasonic techniques yield α_∞ , Λ , Λ' . Measurements in the tube in the low-frequency limit yield the remaining quantities α_0 , k'_0 , α'_0 . (To separate the effects of viscous and thermal parameters, the surface impedance of the sample was measured with a hard baking and with a $\lambda/4$ cavity at the rear face). The dashed lines correspond to the simplification $P=P'=1$, whereas the continuous line assumes the measured values for these factors. The values of M , P , M' , P' , are of order one (resp. 0.95, 0.4, 0.85, 0.45), which explains the excellent agreement obtained with our viscothermal modelling of the relaxation transition.

1. M. Avellaneda and S. Torquato, Phys. Fluids A **3**, 2529-2540 (1991).
2. D.L. Johnson, J. Koplik, R. Dashen, J. Fluid Mech. **176**, 379-402 (1987).
3. S.R. Pride, F.D. Morgan, A.F. Gangi, Phys. Rev. B **47**, 4964-4978 (1993).
4. Y. Champoux and J-F. Allard, J. Appl. Phys. **70**, 1975-1979 (1991).
5. D. Lafarge, P. Lemariniér, J-F. Allard, V. Tarnow, J. Acoust. Soc. Am. **102**, 1995-2006 (1997).
6. A.M. Chapman and J.J.L. Higdon, Phys. Fluids A **4**, 2099-2116 (1992).
7. P. Leclaire, L. Kelders, W. Lauriks, N.R. Brown, M. Melon, B. Castagnède, J. Appl. Phys. **80**, 2009-12 (1996).
8. M. Henry, Thesis Dissertation, Université du Maine (1997).